Radiation Physics and Chemistry 163 (2019) 67–73

Contents lists available at ScienceDirect

Radiation Physics and Chemistry

journal homepage: www.elsevier.com/locate/radphyschem

Photon energy response of LiF:Mg,Ti (MTS) and LiF:Mg,Cu,P (MCP) thermoluminescent detectors: Experimental measurements and microdosimetric modeling

Alessio Parisi[a,b,*], Jérémie Dabin[a], Werner Schoonjans[a], Olivier Van Hoey[a], Patrice Mégret[b], Filip Vanhavere[a]

[a] Belgian Nuclear Research Centre SCK CEN, Mol, Belgium
[b] University of Mons, Faculty of Engineering, Mons, Belgium

ARTICLE INFO

Keywords:
Thermoluminescent detectors
Photon energy response
Microdosimetric d(z) model
PHITS

ABSTRACT

The photon energy response of six thermoluminescent detector types (^{6}LiF:Mg,Ti, ^{7}LiF:Mg,Ti, ^{nat}LiF:Mg,Ti, ^{6}LiF:Mg,Cu,P, ^{7}LiF:Mg,Cu,P and ^{nat}LiF:Mg,Cu,P) was studied in the energy range 12–1250 keV by means of irradiations with different γ-ray sources and X-rays. As expected, for both LiF:Mg,Ti and LiF:Mg,Cu,P detectors, no significant differences were found between the results of detectors with same dopant concentrations but different lithium isotopic enrichment. On the other hand, the type and concentration of dopants influence the photon energy response of the detectors up to 50%. The obtained results were compared with experimental data from literature showing good agreement. In addition, the recently developed Microdosimetric d(z) Model was employed to assess the photon response of these detectors. For microdosimetric calculations performed in the optimal site size of 40 nm (determined in previous investigations with charged particles), a very good agreement was observed between results of the model and the experimental data with an average relative deviation of 3% and 4% for LiF:Mg,Ti and LiF:Mg,Cu,P detectors respectively.

1. Introduction

Radiation detectors based on the thermoluminescence technique are widely used nowadays for the assessment of doses in many fields including personal and ambient dosimetry on Earth, space radiation measurements and cancer radiotherapy applications (McKeever et al., 1995; Olko, 2010, International Commission on Radiological Protection, 2013). While it is intuitive that the response of a luminescent detector depends on the amount of received dose and the materials composing the detector itself, also the way in which this dose is being imparted (i.e. the microscopic pattern of energy deposition) affects strongly its efficiency (Olko, 2007). In case of sparsely ionizing particles such as energetic light particles and photons, the relative efficiency of luminescent detectors is close to 1. On the other hand, the measurement of doses delivered by high linear energy transfer (LET) particles is biased by a strong efficiency decrease (Berger and Hajek, 2008; Bilski and Puchalska, 2010). It follows that an accurate knowledge of these efficiency changes is fundamental for a correct assessment of the measured radiation doses and during the design of dosimeters based on luminescent detectors.

A novel efficiency model, called Microdosimetric d(z) Model (Parisi et al., 2018b) was recently developed for describing the response of luminescent detectors for measuring different radiation qualities. The model is based on microdosimetry (International Commission on Radiation Units and Measurements, 1983) and relates the microscopic pattern of energy deposition with the relative luminescent efficiency of the detectors. The model was successfully benchmarked against experimental data for the two most common materials for thermoluminescent detectors, namely LiF:Mg,Ti and LiF:Mg,Cu,P (Bilski, 2002), in case of exposures to charged particles from ^{1}H to ^{132}Xe in the energy range 3–1000 MeV/u (Parisi et al., 2017c, Parisi et al., 2017d, Parisi et al., 2018b). Furthermore, by combining the response of ^{7}LiF:Mg,Ti and ^{7}LiF:Mg,Cu,P detectors predicted by the Microdosimetric d(z) Model, a new methodology for assessing fluence- and dose-mean unrestricted primary beam LET quantities and relative biological effectiveness (RBE) in proton therapy beams was proposed (Parisi et al., 2019a).

In this work, the validity of the Microdosimetric d(z) Model in assessing the response of luminescent detectors to photons with different energy is investigated. Thus, LiF:Mg,Ti (MTS) and LiF:Mg,Cu,P (MCP)

* Corresponding author. Belgian Nuclear Research Centre SCK CEN, Mol, Belgium.
E-mail address: alessio.parisi@sckcen.be (A. Parisi).

https://doi.org/10.1016/j.radphyschem.2019.05.021
Received 31 August 2018; Received in revised form 15 April 2019; Accepted 10 May 2019
Available online 14 May 2019
0969-806X/

detectors with different lithium isotopic composition were exposed to photons from two γ-ray sources and a X-ray generator and the results were compared with the response of the detectors as predicted by the Microdosimetric d(z) Model.

2. Methodology

2.1. Experimental measurements

2.1.1. Thermoluminescent detectors

The following detectors were employed in this study: ^{6}LiF:Mg,Ti (MTS-6), ^{7}LiF:Mg,Ti (MTS-7), ^{nat}LiF:Mg,Ti (MTS-N), ^{6}LiF:Mg,Cu,P (MCP-6), ^{7}LiF:Mg,Cu,P (MCP-7) and ^{nat}LiF:Mg,Cu,P (MCP-N). All detectors were produced at the Institute of Nuclear Physics (IFJ) in Krakow (Bilski, 2002). ^{nat}LiF:Mg,Ti (MTS-N) detectors are 3.2 x 3.2 × 0.9 mm^3 square chips, while all the other detectors have the form of circular pellets with 4.5 mm diameter and 0.9 mm thickness.

2.1.2. Annealing

Before each exposure, the standard annealing protocols were applied: 10 min at 240 °C followed by fast cooling at −10 °C inside a temperature controlled freezer for LiF:Mg,Cu,P (MCP) detectors and one hour at 400 °C followed by two hours at 100 °C and fast cooling in air to room temperature for LiF:Mg,Ti (MTS) detectors.

2.1.3. Irradiations

All the exposures were performed at the secondary standard calibration laboratory of the Belgian Nuclear Research Centre SCK•CEN using a ^{60}Co γ-ray source (average photon energy 1250 keV), a ^{137}Cs γ-ray source (average photon energy 662 keV) and a X-ray generator. Five ISO 4037 X-ray narrow series were used: N-300, N-150, N-80, N-40 and N-15. The average photon energy was respectively 250, 118, 65, 33 and 12 keV. In all cases, 50 mGy air kerma was delivered. In case of photon exposures using the two γ-ray sources, appropriate build up layers were used to ensure the secondary electron equilibrium. For each radiation quality, five detectors of each type were exposed inside thin transparent polypropylene foils (http://www.esselte.com/it-it/products/archiviazione/buste/busta-quality-esselte_56066, PP, C_3H_6, density = 0.9 g/cm^3, thickness = 55 μm,) in order to simulate the free in air exposure conditions and avoid attenuation and backscattering effects.

2.1.4. Pre-heat

In order to remove the contribution of the unstable low temperature peaks (Parisi et al., 2018a), all detectors were pre-heated for 30 min at 120 °C before the readout.

2.1.5. Background dose assessment

A background detector package was prepared to assess the dose accumulated during the transportation and the storage of the detectors. The background package was composed of five detectors of each type.

2.1.6. Readout

The readout of all detectors was performed using an automatic Harshaw 5500 system. The luminescent signal was recorded heating the detectors with a constant rate of 1 °C/s from room temperature up to 240 or 340 °C for respectively LiF:Mg,Cu,P (MCP) and LiF:Mg,Ti (MTS) detectors.

2.1.7. Individual sensitivity correction

Individual sensitivity factors, obtained irradiating the detectors with a calibrated ^{60}Co γ-ray source at the secondary standard calibration laboratory LNK of the Belgian Nuclear Research Centre SCK•CEN, were determined after the experimental campaign in order to decrease the sensitivity spread among the different detectors. Each individual sensitivity factor was calculated as the ratio between the quantified light signal for a specific detector over the same quantity averaged on all detectors of the same type. The operational protocols used for the determination of the individual sensitivity factors were the same as the ones used for the readout of experimental and background detectors.

2.1.8. Glow curve signal quantification

For all detector types, the quantification of the glow curve was done by means of integrating the light signal over the main peak region of interest (Parisi et al., 2017a). The temperature ranges used were 150 – 248 °C for LiF:Mg,Ti (MTS) detectors and 150 – 240 °C for LiF:Mg,Cu,P (MCP) detectors. The subtraction of the LiF:Mg,Ti inherent background signal due to electronic noise, planchet and black body radiation of the thermoluminescent detector measurable by the photomultiplier was handled accordingly to the methodology described in Parisi et al., 2017b.

2.1.9. Relative response correction

At low photon energy, corrections to the experimental results should be performed in order to take into account the different dose profiles within the detector and its effect on the thermoluminescent light self-absorption during the readout of the detector (Olko, 2002). However, in the photon energy range under investigation (12 to 1250 keV), this correction is negligible (Bilski et al., 1994) and was not applied.

2.2. Microdosimetric modeling of the response of the detectors

In order to allow an easier comparison with literature data, usually presented in the form of relative air kerma response, it was necessary to evaluate a conversion coefficient between air kerma and absorbed dose in lithium fluoride and the relative luminescence efficiency of the detectors. Both factors depend on the energy of the incident photon and the detector type.

2.2.1. Conversion coefficient between air kerma and absorbed dose in the detector

As a first step, Monte Carlo simulations were performed using PHITS and the energy deposition was scored in an air target (mass composition: 0.755 267 ^{14}N, 0.231 781 ^{16}O, 0.012 827 ^{40}Ar and 0.000124 ^{12}C, density = 1.20 479 10^{-3} g/cm^3, thickness = 0.1 mm). The electrons transport cutoff was set to 10 MeV in order to ensure the electronic equilibrium. In order to validate the results of our calculations, the so calculated absorbed dose values per unit of particle were compared with the same quantity assessed using the mass energy absorption coefficients from the mass attenuation and mass energy absorption tables (Hubbell and Seltzer, 2004) of the National Institute of Standards and Technology (NIST, Maryland, United States of America) and knowing the area and the mass of the simulated air volume. The same analysis was then performed in case of ^{7}lithium fluoride target (density = 2.5 g/cm^3, thickness = 0.9 mm) representing our detectors. As a second step, the effect of the presence of dopants on the photon energy dependence of the absorbed dose was investigated repeating the simulations including the nominal dopant concentrations of LiF:Mg,Ti (MTS) and LiF:Mg,Cu,P (MCP) detectors (Bilski, 2002).

2.2.2. Relative luminescence efficiency

The relative luminescence efficiency of the detectors η_{rel}, defined as in Equation (1) as the ratio between intensity of the luminescence signal S per unit of absorbed dose D for the radiation under investigation over the same quantity for a reference radiation (usually γ-rays, X-rays or β-particles), was evaluated using the recently developed Microdosimetric d(z) Model (Parisi et al., 2017c, Parisi et al., 2017d, Parisi et al., 2018a). The model is able to describe the efficiency changes of luminescent detectors for measuring different radiation qualities by relating the simulated dose probability distribution of the specific energy (z, [Gy], International Commission on Radiation Units and Measurements,

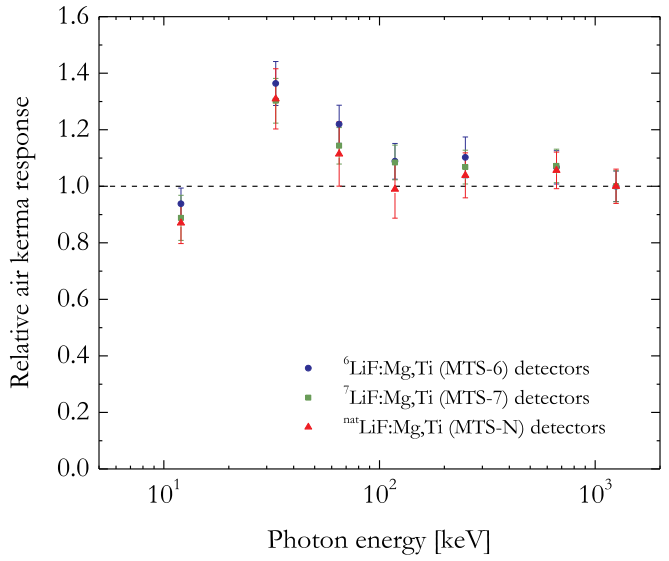

Fig. 1. Relative air kerma response of ^{6}LiF:Mg,Ti (MTS-6), ^{7}LiF:Mg,Ti (MTS-7) and ^{nat}LiF:Mg,Ti (MTS-N) detectors as function of the photon energy.

1983) in nanometric targets with an experimentally determined macroscopic response function characteristic of each detector type.

$$\eta_{rel} = \frac{\left(S/D\right)_{radiation}}{\left(S/D\right)_{reference\ radiation}} \quad (1)$$

The relative luminescence efficiency of the detectors was then evaluated using Equation (2), where d(z) is the dose probability distribution of the specific energy and r(z) is the specific energy response function. Two different response functions were used for the two different detector types under investigation.

$$\eta_{rel} = \frac{\left[\int_0^{+\infty} d(z)\, r(z) dz\right]_{radiation}}{\left[\int_0^{+\infty} d(z)\, r(z) dz\right]_{reference\ radiation}} \quad (2)$$

The dose probability distribution of the specific energy d(z), was assessed by performing simulations with mono-energetic beams

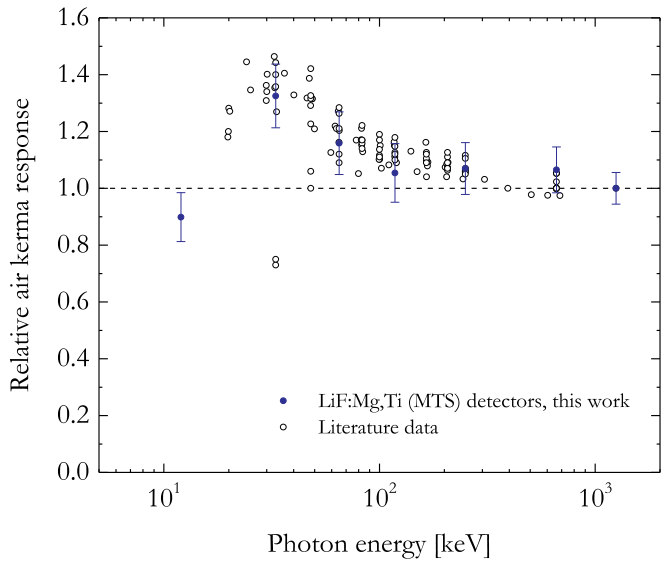

Fig. 2. Comparison between the average relative air kerma photon energy response of all LiF:Mg,Ti (MTS) detectors of this study and experimental data from Sáez-Vergara et al. (1999), Olko (2002), Davis et al. (2003) and Hranitzky et al. (2006).

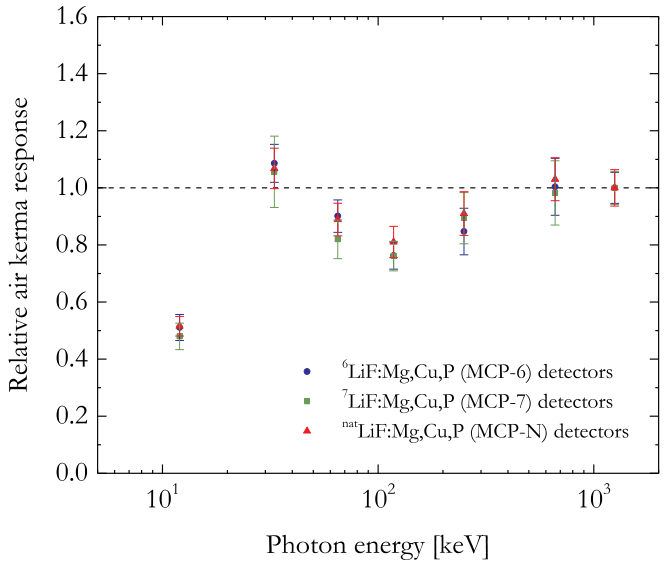

Fig. 3. Relative air kerma response of ^{6}LiF:Mg,Cu,P (MCP-6), ^{7}LiF:Mg,Cu,P (MCP-7) and ^{nat}LiF:Mg,Cu,P (MCP-N) detectors as function of the photon energy.

(energy = 10, 20, 30, 40, 50, 60, 70, 80, 90, 100, 300, 400, 500 600, 662, 700, 800, 900 and 1000 keV) or with a dual-energy (1173.2 and 1332.5 keV) photon beam representing the reference ^{60}Co γ-ray source. The site sizes in which the Monte Carlo simulations were performed ranged from 1 nm to 2 μm. The averaging of the dose probability distribution of specific energy over the detector volume was handled accordingly to the methodology described in Parisi (2018) and Parisi et al., 2018b. All the simulations of Microdosimetric d(z) Model and relative absorbed dose assessment were performed using the Monte Carlo Particle and Heavy Ion Transport code System (PHITS) version 2.82 (Sato et al., 2018). The Electron Gamma Shower version 5 (EGS5) code (Hirayama et al., 2005) was employed for the transport of photons, electrons and positions.

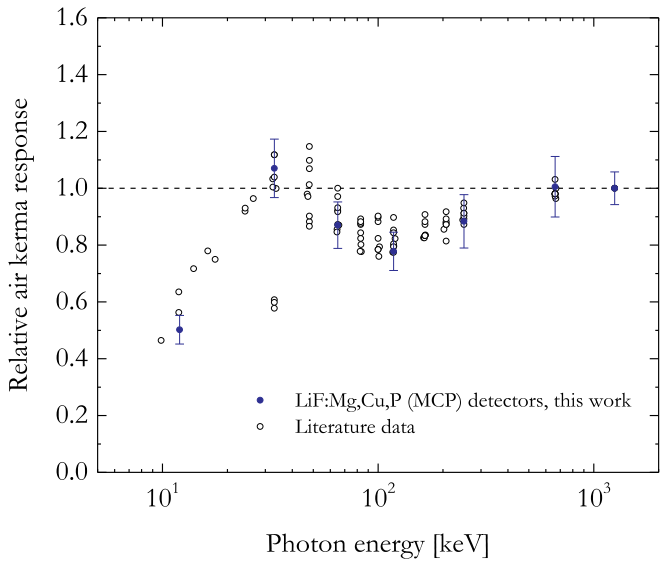

Fig. 4. Comparison between the average relative air kerma photon energy response of all LiF:Mg,Cu,P (MCP) detectors of this study and experimental data from Sáez-Vergara et al. (1999), Olko (2002), Davis et al. (2003) and Hranitzky et al. (2006).

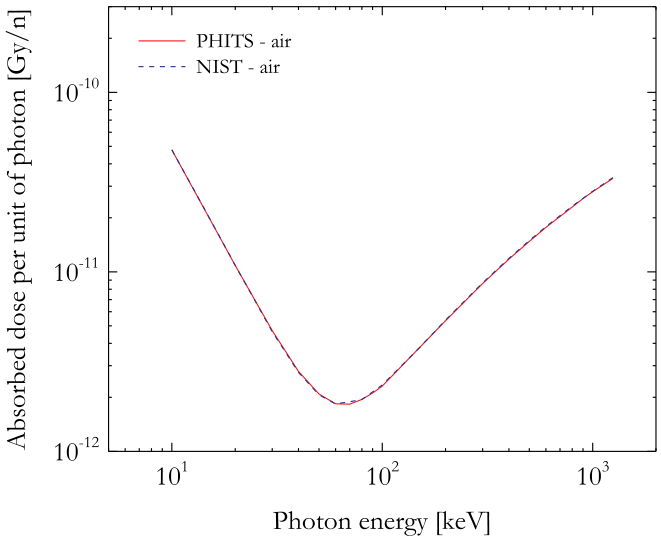

Fig. 5. Comparison between the energy dependence of the absorbed dose values in air per unit of photon evaluated by using PHITS or NIST.

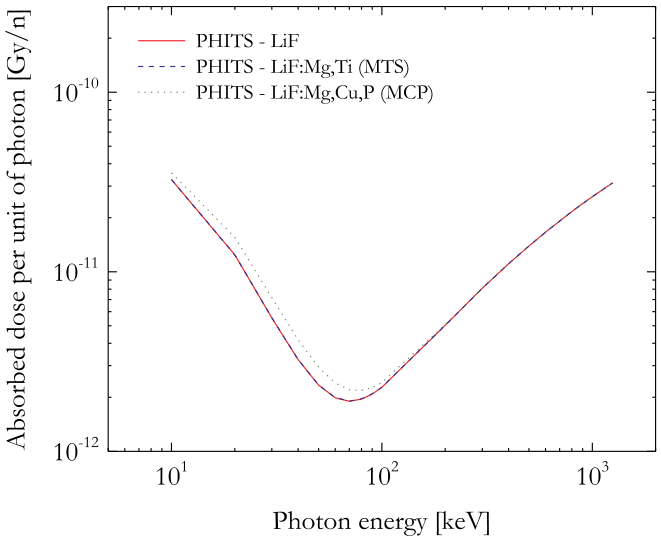

Fig. 7. Effect of including the detector dopants on the energy dependence of the absorbed dose values in lithium fluoride per unit of photon.

3. Results and discussion

3.1. Experimental results

3.1.1. LiF:Mg,Ti (MTS) detectors

Fig. 1 compares the relative air kerma response of ^{6}LiF:Mg,Ti (MTS-6), ^{7}LiF:Mg,Ti (MTS-7) and ^{nat}LiF:Mg,Ti (MTS-N) detectors as function of the photon energy. The results are normalized to the ones stemming from the ^{60}Co γ-ray exposure. Here and all the following graphs, the vertical error bars represent a combined standard uncertainty including the statistical spread of the detectors, the error propagation of the statistical spread in case of the reference ^{60}Co γ-ray exposure and a cumulative uncertainty in the delivered relative dose. The latter term includes the uncertainty in the reference irradiation and the photon energy under investigation and was assessed to be 5%. As expected, the relative response no relevant differences were found between the results of detectors with different lithium isotopic concentrations. The air kerma response of the detectors is characterized by the presence of a local maximum (~1.3) for photon energies between 30 and 40 keV. At lower energies, a sharp decrease is observed down to a value of 0.5 for 10 keV photons.

In Fig. 2, the average relative values of the relative air kerma response of these three LiF:Mg,Ti detector types (MTS-6, MTS-7 and MTS-N) are compared with experimental data from Sáez-Vergara et al. (1999), Olko (2002), Davis et al. (2003) and Hranitzky et al. (2006). Notwithstanding the large spread in the literature data, a good agreement seems to be present. The large spread in the literature data can be due to differences in the protocols used for the glow curve signal quantification, the thermal treatments performed on the detectors, the reading system used and the manufacturer of the detectors. Furthermore, the material composing the holder used for the simulation of the free in air conditions was proven to play a significant role, leading to differences up to 50% in the relative air kerma response (Sáez-Vergara et al., 1999).

3.1.2. LiF:Mg,Cu,P (MCP) detectors

The relative air kerma responses of ^{6}LiF:Mg,Cu,P (MCP-6), ^{7}LiF:Mg,Cu,P (MCP-7) and ^{nat}LiF:Mg,Cu,P (MCP-N) detectors are plotted in Fig. 3 as function of the photon energy. As in case of

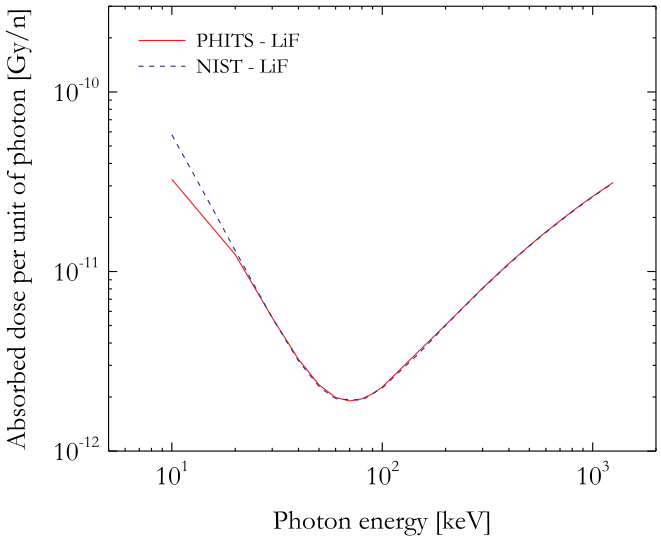

Fig. 6. Comparison between the energy dependence of the absorbed dose values in lithium fluoride per unit of photon evaluated by using PHITS or NIST.

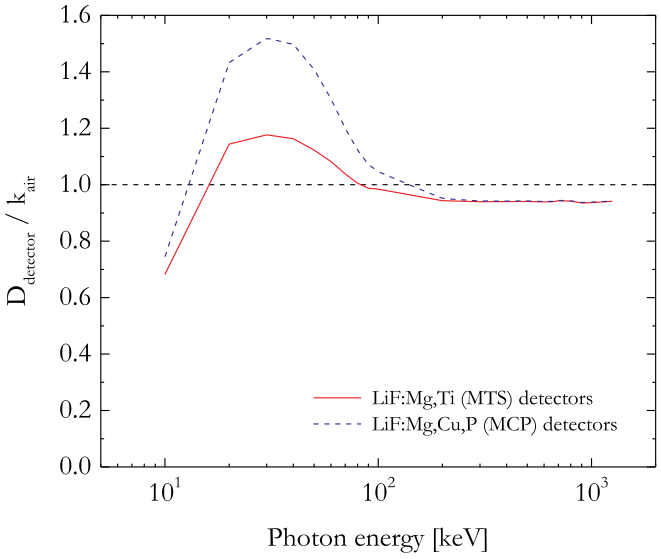

Fig. 8. Ratio between the absorbed dose in the detector and the air kerma as function of the photon energy.

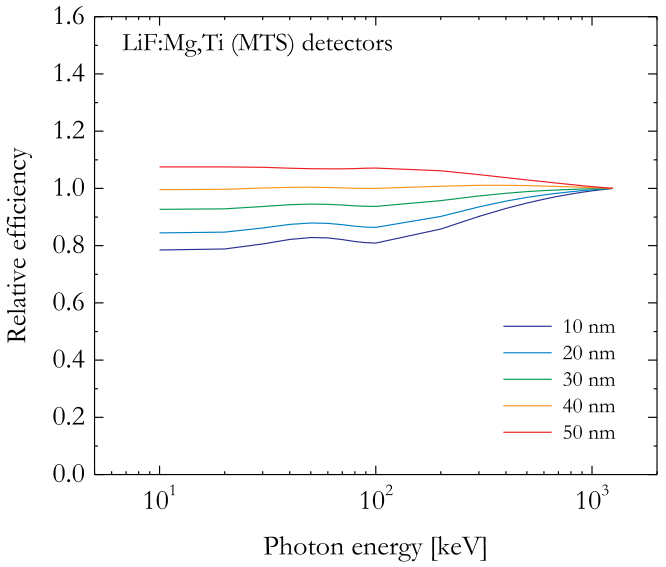

Fig. 9. Effect of changing the site size on the calculated relative efficiency values of LiF:Mg,Ti (MTS) detectors exposed to photons.

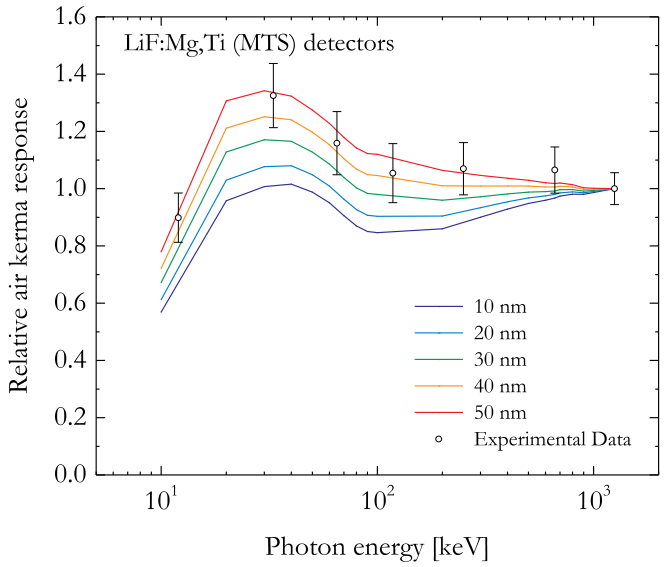

Fig. 11. Effect of changing the site size on the calculated relative air kerma response of LiF:Mg,Ti (MTS) detectors as function of the photon energy.

LiF:Mg,Ti (MTS) detectors, the results for the three lithium isotopic compositions agree within the statistical uncertainties. Starting from a value of 1 in case of the reference ^{60}Co γ-ray source (1250 keV), a decrease in the relative air kerma response is observed with the decrease of the photon energy down to a local minimum of approximately 0.8 for a photon energy of around 100 keV. An additional decrease of the photon energy is associated with an increase of the relative response up to a local maximum of roughly 1.1 for 30 keV photons. At lower energies, a a sharp decrease in the relative air kerma response was found down to approximately 0.5 for 10 keV photons. In Fig. 4, the average air kerma response of all LiF:Mg,Cu,P (MCP) detectors is compared with experimental data from Sáez-Vergara et al. (1999), Olko (2002), Davis et al. (2003) and Hranitzky et al. (2006), showing a good agreement.

3.2. Microdosimetric modeling of the response of the detectors

3.2.1. Validation of the PHITS simulations

Fig. 5 compares the absorbed dose in air per unit of photon in case of PHITS calculations the NIST based approach. The latter parameter was found to initially decrease with the increase of the photon energy, starting from a value of 4.78 10^{-11} Gy for a photon energy of 10 keV down to a local minimum of 1.83 10^{-12} Gy at 60-70 keV and then increase up to a value of 3.32 10^{-11} for 1250 keV photons. As it can be seen, a very good agreement between the two data series is present, with an average relative deviation of 0.8%.

Similarly, also in case of absorbed dose in lithium fluoride (Fig. 6), a local minimum (1.90 10^{-12} Gy) was found for photons with energy of approximately 70 keV. The agreement between the results of the PHITS and NIST based approaches is very good for photon energies above 20 keV, with an average relative deviation of 0.9%. At lower energies the PHITS results seem to underestimate the NIST ones. For instance, in case of 10 keV photons, the NIST results (5.78 10^{-11} Gy) are approximately 1.8 times higher than the PHITS ones (3.26 10^{-11} Gy). This happens because in the PHITS simulations the real thickness of the detector (0.9 mm of lithium fluoride) was included, while NIST values are relative to point quantities. Consequently, in the NIST approach, the

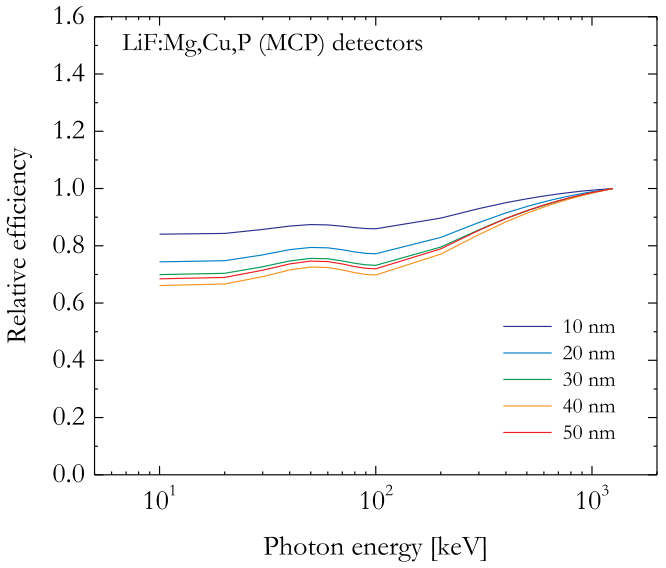

Fig. 10. Effect of changing the site size on the calculated relative efficiency values of LiF:Mg,Cu,P (MCP) detectors exposed to photons.

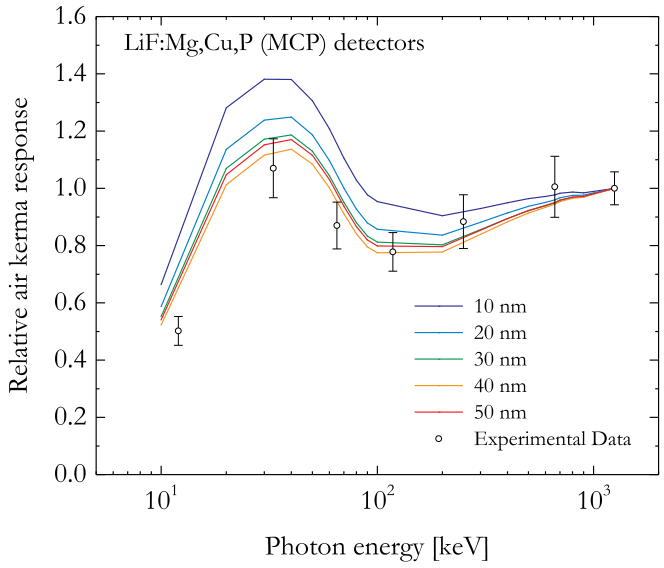

Fig. 12. Effect of changing the site size on the calculated relative air kerma response of LiF:Mg,Cu,P (MCP) detectors as function of the photon energy.

beam attenuation was not taken into account. This explains the differences between the results of the PHITS and NIST based approaches with the former one being more appropriate for this kind of calculations.

3.2.2. Conversion coefficient between air kerma and absorbed dose in the detector

The results plotted in Fig. 7 show that the inclusion of LiF:Mg,Ti (MTS) dopants plays a negligible role in the assessment of the absorbed dose. On the other hand, because of their higher concentrations, the dopants of LiF:Mg,Cu,P (MCP) detectors affect the results of simulations for photon energy below 100 keV up to a maximum value of 30% in case of 30–40 keV photons.

The ratio between the absorbed dose in the detector and the air kerma is plotted in Fig. 8 as function of the photon energy. For both detector types, this ratio has a constant value of approximately 0.94 for energies above 200 keV. For lower energies, an increase of this quantity is observed with the decrease of the photon energy until a local maximum approximately around 30-40 keV. The value of the local maximum for LiF:Mg,Cu,P (MCP) detectors is higher than in case of LiF:Mg,Ti (MTS) detectors, being respectively 1.5 and 1.15. The latter difference is due to the higher concentration of dopants of the first detector type. Finally, below 20 keV, a decrease of the ratio between absorbed dose in the detector and air kerma is observed with the decrease of the photon energy down to a value of roughly 0.7 for both detector types.

3.2.3. Relative luminescence efficiency

Figs. 9 and 10 compare the results of the model in case of respectively LiF:Mg,Ti (MTS) and LiF:Mg,Cu,P (MCP) detectors for calculations performed in site sizes ranging from 10 to 50 nm, plotted as function of the photon energy. Changing the site size has a different effect on the calculated efficiency of the two detector types. In case of LiF:Mg,Ti (MTS) detectors an increase in the dimension of the site size induces an increase in the calculated relative efficiency values especially for low energy photons. On the other hand, for LiF:Mg,Cu,P (MCP) detectors an opposite behavior is observed: an increase in the simulated site size induces a decrease un the calculated values. However, an exception to this trend is represented by the results of 50 nm site size which are slightly higher than the 40 nm ones. As for LiF:Mg,Ti (MTS) detectors, the most relevant differences occur in case of low energy photons.

3.2.4. Relative air kerma response

Combining the results of Figs. 8–10, the relative air kerma response of the detectors was evaluated. The absorbed dose trends used for these calculations are the ones relative to the simulations performed including the appropriate dopant concentrations for both detector types. The results were normalized to the ones of the photons from the ^{60}Co γ-source (average photon energy = 1250 keV) and compared in Figs. 11 and 12 with the experimental data of Section 3.1 this manuscript.

Notwithstanding the large statistical spread in experimental data, the best agreement (quantified as minimum average relative deviation) between the results of the Microdosimetric d(z) Model and the experimental ones was found in case of calculations performed in a site size of 40 nm for both LiF:Mg,Ti (MTS) and LiF:Mg,Cu,P (MCP) detectors with an average relative deviation of 3% and 4% respectively. It has to be remembered that 40 nm was the site size which was found to be the optimal one for charged particles from ^{1}H to ^{132}Xe in the energy range 3–1000 MeV/u (Parisi et al., 2017c, Parisi et al., 2017d, Parisi et al., 2018b).

4. Conclusions

Six types of thermoluminescent detectors were exposed to photons in the energy range 12–1250 keV. It was found that the lithium isotopic composition of the detectors is not affecting its relative air kerma photon energy response. On the other hand, differences up to 50% were found between the relative air kerma response of LiF:Mg,Ti (MTS) and LiF:Mg,Cu,P (MCP) detectors. By using the Microdosimetric d(z) Model, the response of the two detectors was assessed and compared with the experimental results. A very good agreement was found in case of simulations performed in a microdosimetric site size of 40 nm, which represents the optimal value previously observed for relative efficiency determination in case of charged particle exposures (from ^{1}H to ^{132}Xe ions). These results confirm the goodness and flexibility of the Microdosimetric d(z) Model in describing the response of luminescent detectors. The model can be then employed for the calculation of efficiency correction factors in case of measurements performed in known photon energy fields. As next step, the model could be used for the assessment of the response of these detectors for measuring and exotic radiation qualities such as pions, kaons, tauons and antimatter.

References

Berger, T., Hajek, M., 2008. TL-efficiency—overview and experimental results over the years. Radiat. Meas. 43 (2–6), 146–156.

Bilski, P., Olko, P., Burgkhardt, B., Piesch, E., Waligórski, M.P.R., 1994. Thermoluminescence efficiency of LiF: Mg, Cu, P (MCP-N) detectors to photons, beta-electrons, alpha particles and thermal neutrons. Radiat. Protect. Dosim. 55 (1), 31–38.

Bilski, P., 2002. Lithium fluoride: from LiF: Mg, Ti to LiF: Mg, Cu, P. Radiat. Protect. Dosim. 100 (1–4), 199–205.

Bilski, P., Puchalska, M., 2010. Relative efficiency of TL detectors to energetic ion beams. Radiat. Meas. 45 (10), 1495–1498.

Davis, S.D., Ross, C.K., Mobit, P.N., der Zwan Van, L., Chase, W.J., Shortt, K.R., 2003. The response of lif thermoluminescence dosemeters to photon beams in the energy range from 30 kV x rays to 60Co gamma rays. Radiat. Protect. Dosim. 106 (1), 33–43.

Hirayama, H., Namito, Y., Nelson, W.R., Bielajew, A.F., Wilderman, S.J., 2005. The EGS5 Code System (No. SLAC-R-730).

Hranitzky, C., Stadtmann, H., Olko, P., 2006. Determination of LiF: Mg, Ti and LiF: Mg, Cu, P TL efficiency for X-rays and their application to Monte Carlo simulations of dosemeter response. Radiat. Protect. Dosim. 119 (1–4), 483–486.

Hubbell, J.H., Seltzer, S.M., 2004. Tables of X-Ray Mass Attenuation Coefficients and Mass Energy-Absorption Coefficients from 1 keV to 20 MeV for Elements Z = 1 to 92 and 48 Additional Substances of Dosimetric Interest. National Institute of Standards and Technology, Gaithersburg, MD Available online at: http://physics.nist.gov/xaamdi, version 1.4.

International Commission on Radiation Units and Measurements, 1983. ICRU Report 36. Microdosimetry.

International Commission on Radiological Protection, 2013. ICRP Publication 123. Assessment of Radiation Exposure of Astronauts in Space.

McKeever, S.W., Moscovitch, M., Townsend, P.D., 1995. Thermoluminescence Dosimetry Materials: Properties and Uses.

Olko, P., 2002. Microdosimetric Modelling of Physical and Biological Detectors (Habilitation Thesis). Henryk Niewodniczański Institute of Nuclear Physics.

Olko, P., 2007. Microdosimetry, track structure and the response of thermoluminescence detectors. Radiat. Meas. 41, S57–S70.

Olko, P., 2010. Advantages and disadvantages of luminescence dosimetry. Radiat. Meas. 45 (3–6), 506–511.

Parisi, A., Van Hoey, O., Mégret, P., Vanhavere, F., 2017a. The influence of the dose assessment method on the LET dependence of the relative luminescence efficiency of LiF:Mg,Ti and LiF:Mg,Cu,P. Radiat. Meas. 98, 34–40.

Parisi, A., Van Hoey, O., Mégret, P., Vanhavere, F., 2017b. Deconvolution study on the glow curve structure of LiF:Mg,Ti and LiF:Mg,Cu,P thermoluminescent detectors exposed to 1H, 4He and 12C ion beams. Nucl. Instrum. Methods Phys. Res. Sect. B Beam Interact. Mater. Atoms 407, 222–229.

Parisi, A., Van Hoey, O., Vanhavere, F., 2017c. Microdosimetric modeling of the relative luminescence efficiency of LiF:Mg,Ti (MTS) detectors exposed to charged particles. Radiat. Protect. Dosim. 1–4.

Parisi, A., Van Hoey, O., Mégret, P., Vanhavere, F., 2017d. Microdosimetric Modeling of the Relative Luminescence Efficiency of LiF:Mg,Cu,P (MCP) Detectors Exposed to Charged Particles. Radiation Protection Dosimetry published online.

Parisi, A., 2018. Space and Hadron Therapy with Luminescent Detectors: Microdosimetric Modeling and Experimental Measurements. PhD Thesis, Polytech of Mons. .

Parisi, A., De Freitas Nascimento, L., Van Hoey, O., Mégret, P., Kitamura, H., Kodaira, S., Vanhavere, F., 2018a. Low temperature anomaly of LiF:Mg,Cu,P (MCP) thermoluminescent detectors exposed to 1H and 4He ions. Radiat. Meas. 119, 155–165.

Parisi, A., Van Hoey, O., Mégret, P., Vanhavere, F., 2018b. Microdosimetric specific energy probability distribution in nanometric targets and its correlation with the efficiency of thermoluminescent detectors exposed to charged particles. Radiat. Meas. 123, 1–12.

Parisi, A., Chiriotti, S., De Saint-Hubert, M., Van Hoey, O., Vandevoorde, C., Beukes, P., de Kock, E., Symons, J., Nieto Camero, J., Slabbert, J.P., Mégret, P., Debrot, E., Bolst, D., Rosenfeld, A., Vanhavere, F., 2019a. A novel methodology to assess linear energy transfer and relative biological effectiveness in proton therapy using pairs of

differently doped thermoluminescent detectors. Phys. Med. Biol. 64, 085005.
Sáez-Vergara, J.C., Romero, A.M., Ginjaume, M., Ortega, X., Miralles, H., 1999. Photon energy response matrix for environmental monitoring systems based on LiF: Mg, Ti and hypersensitive phosphors (LiF: Mg, Cu, P and a-Al2O3: C). Radiat. Protect. Dosim. 85 (1–4), 207–211.
Sato, T., Iwamoto, Y., Hashimoto, S., Ogawa, T., Furuta, T., Abe, S.I., Kai, T., Tsai, P.E., Matsuda, N., Iwase, H., Shigyo, N., 2018. Features of particle and Heavy ion transport code system (PHITS) version 3.02. J. Nucl. Sci. Technol. 55 (6), 684–690.